Eur. Phys. J. B **43**, 503–507 (2005)
DOI: 10.1140/epjb/e2005-00083-9

THE EUROPEAN PHYSICAL JOURNAL B

Perspectives in the characteristics and applications of Tauc-Lorentz dielectric function model

H. Chen and W.Z. Shen[a]

Laboratory of Condensed Matter Spectroscopy and Opto-Electronic Physics, Department of Physics, Shanghai Jiao Tong University, 1954 Hua Shan Road, Shanghai 200030, P.R. China

Received 8 December 2004 / Received in final form 18 January 2005
Published online 30 March 2005 – © EDP Sciences, Società Italiana di Fisica, Springer-Verlag 2005

Abstract. We explore inherent characteristics of Tauc-Lorentz (TL) dielectric function model [Appl. Phys. Lett. **69**, 371 (1996)] on the basis of relevant optical-constant data in the literature. It is found that the (single or multiple) TL model is strongly related to the one-oscillator Wemple-DiDomenico (WD) model [Phys. Rev. B **3**, 1338 (1971)]. New physical significance has been attached to the transition energy parameter of the TL model in terms of the WD model. We have also attempted to extend the applications of the TL model to evaluating specific bond density in various semiconductors, proposing a criterion for judging whether the quantum size effect is prominent or not within crystalline/amorphous mixed-phase materials, and obtaining information about mass density and coordination number of the samples investigated. These perspectives directly provide the possibility of deeper and wider usage of the TL model in many other covalent and ionic materials.

PACS. 78.20.Bh Theory, models, and numerical simulation – 78.20.Ci Optical constants (including refractive index, complex dielectric constant, absorption, reflection and transmission coefficients, emissivity)

It is well known that dielectric function models are crucial in extracting optical constants (refractive index n and extinction coefficient k) of a substance as a function of photon energy (E) from optical transmission/reflection or spectroscopic ellipsometry measurements. The Tauc-Lorentz (TL) model [1], which was firstly but empirically proposed by Jellison and Modine in 1996, can overcome some intrinsic shortcomings of its counterpart, i.e., Forouhi-Bloomer (FB) model [2], and has been currently employed for several kinds of amorphous [3–9], polycrystalline [10,11], and crystalline/amorphous (c^-/a^-) mixed-phase materials [12–14]. Its imaginary part of dielectric function $\varepsilon_{2TL}(E)$ is established through multiplying the equation of the classical Lorentz oscillator by the expression of the Tauc joint density of states [1]:

$$\varepsilon_{2TL}(E) = 2n(E)k(E) = \begin{cases} \frac{A_{TL}E_{0TL}C_{TL}(E-E_{TL})^2}{(E^2-E_{0TL}^2)^2+C_{TL}^2E^2}\cdot\frac{1}{E}, E > E_{TL}, \\ 0, E \le E_{TL}. \end{cases} \quad (1)$$

The real part of the dielectric function $[\varepsilon_{1TL}(E) = n^2(E)-k^2(E)]$ is obtained by Kramers-Kronig integration. There are five fitting parameters in the above single TL model [1,13]: the transition-matrix-element related A_{TL}, transition energy E_{0TL}, broadening parameter C_{TL}, band gap E_{TL}, and constant $\varepsilon_{1\infty}$ (appearing in the expanded form of ε_{1TL}). The multiple TL model which is the sum of several single-TL terms, e.g., double TL (2TL) [10,11], generally corresponds to multi-transitions. People are used to extracting optical constants of semiconductors and dielectrics by means of the TL model, but pay little attention to its inherent characteristics and further applications.

It should be noted that the TL model includes only interband transitions; any defect absorption, intraband absorption, or Urbach tail absorption is explicitly ignored in it [1]. Four modified versions of the TL model have been proposed so far to remedy some of its limitations, i.e., generalized TL expression [15], TL with the inclusion of Urbach tail (denoted as TLU model) [16], TLU model with the assumption of continuous first derivative of dielectric function [17], and TL model with empirical extension of the non-zero $\varepsilon_{2TL}(E)$ to the whole spectral range [13]. However, due to the empirical nature of the TL model, the single or multiple TL models without any modifications are usually capable to reproduce the experimental data very well even below the optical band gap (see Refs. [1,5,6,10,11] for supporting examples). This is because that the components of Lorentz oscillator and Tauc

[a] e-mail: wzshen@sjtu.edu.cn

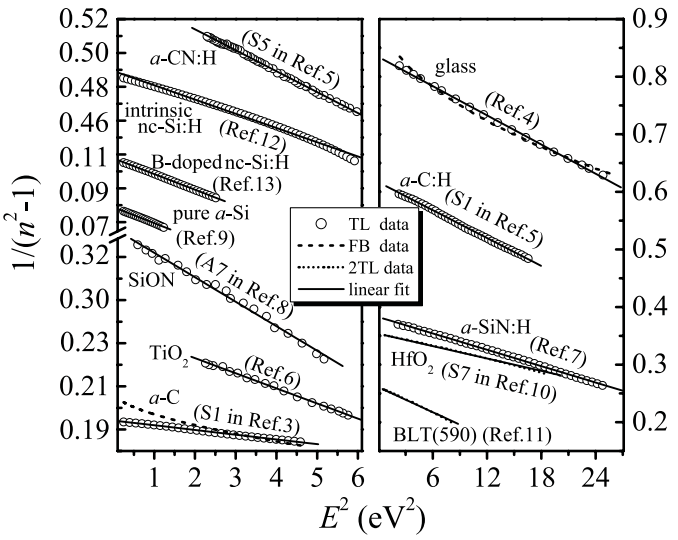

Fig. 1. Plots of factor $(n^2-1)^{-1}$ versus E^2 for the subgap refractive indices n (open circles: yielded by the single TL model; dashed curves: yielded by the FB model; dotted curves: yielded by the double TL model; solid lines: linear fits) of various semiconductors and dielectrics.

joint density of states in $\varepsilon_{2TL}(E)$ may describe the below-band-gap and above-band-gap absorption, respectively. The tradeoff between these two components results in the reduction of the nominal band gap E_{TL} (TL gap) relative to the true optical band gap E_g, when the TL model fits to real data. The absorption below E_g is actually embodied within the photon energy range between E_{TL} and E_g to some extent. The TL gap is thus a mathematical gap rather than a real physical one. Nevertheless, as compared with the FB model, the TL model can reflect more correct optical responses of matter, especially the "subgap" (mainly below E_g, sometimes below E_{0TL}) refractive index, which has been scarcely realized so far to provide insights into material microstructure.

In this article, we examine the subgap refractive-index behavior (magnitude and dispersion) deduced from the TL fitting parameters available in the literature and find that the TL model is strongly related to the one-oscillator Wemple-DiDomenico (WD) model [18] through which we obtain information about the material microstructure. New physical significance within the TL model can thus be revealed; deeper and wider applications of the TL model are possible to be extended and predicted.

Figure 1 shows typically the TL-yielded subgap $n(E)$ (open circles and dotted curves) plotted by way of $1/(n^2-1)$ versus E^2 for various semiconductors and dielectrics such as a-C [3], glass [4], a-C:H [5], nitrogen-doped a-C:H (a-CN:H) [5], high-k dielectric TiO_2 [6] and HfO_2 [10], ferroelectric $Bi_{3.25}La_{0.75}Ti_3O_{12}$ (BLT) [11], a-SiN:H [7], silicon oxynitride (SiON) [8], pure a-Si [9] and a-Si:H [14], intrinsic [12] and B-doped [13] nanocrystalline Si:H (nc-Si:H), polymorphous Si:H [14] and protocrystalline Si:H (proto-Si:H) [14] films. As indicated by good linear fits (solid lines) in Figure 1, we find that no matter which kind of TL model has been used (i.e., single or multiple) and no matter which kind of form the investigated materials present (i.e., amorphous, polycrystalline, or c^-/a^- mixed-phase), all of the TL-yielded subgap $n(E)$ in these materials obey remarkably the one-oscillator WD model of the form [18]

$$n^2(E) - 1 = E_d E_0 / \left(E_0^2 - E^2\right), \qquad (2)$$

where E_0 is the single oscillator energy, and E_d is the dispersion energy (some values of E_0 and E_d for Si-based materials are listed in Table 1). In contrast, the FB-yielded subgap $n(E)$ (dashed curves) cannot be well described by the WD model, as demonstrated by two examples in Figure 1, i.e., a-C and glass, whose TL-yielded subgap $n(E)$ turn out to be consistent with their nature [19]. Thus the refractive-index behavior which obeys strikingly the WD model in the subgap region is believed to be inherent within the TL model instead of the FB model. This conclusion is one of the main new findings in current work and then we are able to infer as follows: In general, single TL corresponds to one dominant interband optical transition, double TL corresponds to two transitions, and so on. Since single TL model is related to one-oscillator WD model, and multiple-oscillator WD model has been demonstrated to be equivalent to one-effective-oscillator WD model [18], thus any multiple TL model is always related to one-oscillator WD model.

The origin why the TL model is strongly related to the WD model is twofold: (i) the TL model reveals more reliable dielectric response than the FB model in the subgap region, where the refractive-index behavior of large groups of matter obeys Sellmeier equation of the form $n^2(E) - 1 = (A_0 - 1) + B_0/(C_0^2 - E^2)$, with A_0, B_0 and C_0 the fitting constants. E^2 is generally much less than C_0^2 in the subgap region, Sellmeier equation is thus approximately equivalent to WD expression by using $(A_0-1)+B_0/(C_0^2-E^2) \approx ((A_0-1)C_0^2+B_0)/(C_0^2-E^2)$. (ii) When $E < E_g$ or when E_{TL} is small enough as compared with E, the TL model will approach the classical Lorentz oscillator model [1], whose expression for the real part of dielectric function $\varepsilon_1(E)$ turns out be equivalent to the Sellmeier equation and subsequently to WD expression after using $\varepsilon_1(E) = n^2(E)$ and neglecting the broadening term. We adopt the WD model here rather than the Sellmeier equation, because WD parameters have fundamental physical significance and can provide new insights into the microstructure of matter [18].

Now we tentatively discuss new physical significance implicit within the TL model in terms of the WD model. Parameter E_0 is the energy of the effective oscillator, which is typically near the main peak of the imaginary part of dielectric function ε_2. It has been extended to measure the energy difference between the "centers of gravity" of the valence and conduction bands, indicative of an average gap of the material [20]. This average gap gives quantitative information on the "overall" band structure, differing from the conventional optical gap such as Tauc gaps [1] which probes optical properties near the fundamental band gap of the material. In the successful usage

Table 1. Transition energy E_{0TL} of the single TL model and refractive-index dispersion parameters revealed by the WD model for various silicon-based materials, together with the fitting energy ranges for equation (2).

Sample	E_{0TL} (eV)	E_0 (eV)	E_d (eV)	Energy Range (eV)
c-Si [18]	–	4.0	44.4	–
Intrinsic nc-Si:H [12]	6.508	7.902	16.204	0.50–2.43
B-doped nc-Si:H [13]	3.312	3.412	31.687	0.50–1.58
pure *a*-Si [9]	3.40	2.873	36.404	0.50–1.11
a-Si:H [14] 50 °C	3.68	3.447	35.506	0.50–1.70
100 °C	3.66	3.498	36.791	0.50–1.70
200 °C	3.62	3.477	38.923	0.50–1.70
250 °C	3.60	3.444	41.306	0.50–1.70
proto-Si:H [14]: 93 Pa	3.69	3.636	40.804	0.50–1.80
80 Pa	3.69	3.662	39.401	0.50–1.82
53 Pa	3.78	3.669	38.657	0.50–1.82

of single TL model (usually for amorphous materials), the transition energy parameter E_{0TL}, which is closely comparable to E_0 and the peak energy of ε_2, reflects such overall band structure information. In addition, localized states near the conduction or valence band (i.e., tail states) may have a strong effect on the optical absorption and subsequently on the optical gap, whereas if they have a small polarizability, they will increase the Urbach tail but have little effect on the average gap [20]. In cases of multiple TL model (generally for multi-transition amorphous, polycrystalline materials), multiple E_{0TL} parameters correspond roughly to different transition energies, or even critical points such as E_1; however, we can still resort to E_0 for aforementioned "overall" band structure information.

Another important WD parameter E_d, which is a measure of the strength of interband optical transitions and nearly independent of E_0, is found to follow a simple relationship $E_d = \beta N_c Z_a N_e$ in a variety of crystalline covalent and ionic solids and liquids. N_c is the coordination number of the cation nearest neighbor to the anion, Z_a, N_e, β are constants [18]. In diamond-type structure of *c*-Si, $N_c = 4$, with E_0 and E_d given in Table 1. The WD model was extended to amorphous semiconductor and glasses [19], by proposing a relation $E_d^a/E_d^x = (\rho^a/\rho^x)(N_c^a/N_c^x)$, where ρ is the mass density, and a and x refer to amorphous and crystalline forms, respectively. This relation is also expected to retain for the mixed-phase materials like nc-Si:H, with the possible distinction of constant β. Therefore, E_d mainly reveals information about density and coordination number.

Let us then take silicon-based materials as examples to investigate deeper and wider applications of the TL model in combination with the WD model. Table 1 lists the fitted one-oscillator WD parameters E_0 and E_d for these samples via the TL-yielded subgap $n(E)$ data. It is evident that E_{0TL} is closely comparable to E_0 and both exhibit nearly the same trend with the variation of growth conditions. These observations can also give new insights into the specific bond density of the samples. For instance, E_{0TL} of *a*-Si:H decreases with increasing the substrate temperature T_s, implying hydrogen content $C_{\rm H}$ in these *a*-Si:H decreases with increasing T_s, since the Si-H bond is known to be stronger than the Si-Si bond and hence an increased Si-H bond density aids E_{0TL} to increase. This conclusion is in good agreement with the $C_{\rm H}$ values obtained by the accurate elastic recoil detection analysis [14].

As to c^-/a^- mixed-phase materials such as nc-Si:H and proto-Si:H, where the nanocrystals (i.e., grains) are embedded in an amorphous silicon matrix [13,14], quantum size effect (QSE) may play a role in determining their optical properties. A size-related criterion about judging the degree of QSE was once used, asserting that the grain size should be less than 5 nm for considerable QSE in nc-Si:H [21]. Nevertheless, other factors like grain shape, grain spacing, and size distribution also have a great effect on QSE, thus obscure the judgment regarding whether the QSE is prominent or not in the sample studied. Fortunately, based on the WD model, we can propose another criterion of QSE for c^-/a^- mixed-phase substances from the viewpoint of $\varepsilon_1(E)$: the reduction in subgap refractive index of the material investigated is primarily ascribed to the average gap E_0 expansion, which proves to be interestingly equivalent to the method of reference [22]. When E_0 is larger than that of *c*-Si (i.e., 4.0 eV) it implies prominent QSE, otherwise it implies negligible QSE there. E_{0TL} of single TL model can also reveal similar qualitative information about QSE, since it approximates E_0. This criterion supplies us straightforward and convenient experience for judging the degree of QSE from either E_0 or E_{0TL}. For example, the TL-yielded E_0 of 7.902 eV for the intrinsic nc-Si:H (Table 1), which deviates significantly from that of *c*-Si, indicates evident QSE. This is reasonable since the grain size of the intrinsic nc-Si:H is only about 3.5 nm. Similarly, the single-TL-fitted E_{0TL} of 4.643 eV in a c^-/a^- Si nanostructure [near the relevant peak energy of ε_2 (4.56 eV) in curve (v)] corroborates

the theoretically-expected sizable QSE [23]. In contrast, QSE is not evident in the B-doped nc-Si:H [13] and proto-Si:H [14] (Tab. 1); the variation of E_0 and E_{0TL} with growth conditions in proto-Si:H can be further correlated with different Si-H bond densities [14].

Mass density information can be deduced from E_d. E_d in pure a-Si and a-Si:H are obviously smaller than that in their crystalline analog (see Tab. 1), due to their under-coordination related to dangling bonds and density deficit associated with voids. The TL-yielded E_d for the intrinsic nc-Si:H sample discussed above is strikingly less than those of c-Si and a-Si:H, indicating large amount of voids within the sample, since the reduction of E_d due to the under-coordination relative to c-Si is only 3–5% even in void-free pure a-Si [24] and negligible here. This justifies that the intrinsic nc-Si:H sample is porous in nature [12]. Moreover, E_d of a-Si:H deposited at different T_s [14] increases with T_s (Tab. 1), which is consistent with the accurate density measurements in these a-Si:H thin films [14] and can be well explained from the viewpoint of growth mechanism: the annealing effect induced by the increase of T_s will remove some dangling bonds and decrease the amount of voids and hydrogen in the a-Si:H, thus resulting in the dominant increase of the density.

Also, illustration of the variation of average coordination number N_c revealed by E_d can be found in proto-Si:H deposited under different gas pressures P. As opposite to the variation of E_0, E_{0TL} (Tab. 1), mass density ρ, calculated crystallinity X_c and hydrogen content $C_{\rm H}$ [14], the E_d of these proto-Si:H decreases with the reduction of P, implying the decrease of N_c with decreasing P. The proto-Si:H can be treated as a mixture of two components, i.e., c-Si and a-Si:H. If the amorphous phase was under-coordinated (i.e., corresponding to dangling bonds, $N_c < 4$) relative to crystalline phase ($N_c = 4$) in the proto-Si:H, the increase of the average N_c with X_c would be expected on the whole. Since this is not the case, as indicated by the tabulated E_d together with ρ results, it is necessary to invoke the concept of "floating bonds" proposed by Pantelides [25] for over-coordinated defects ($N_c > 4$) within the amorphous tissue of these proto-Si:H. It can be well understood that with increasing X_c for these films, more floating bonds would be passivated by hydrogen during film growth, leading to the increase of $C_{\rm H}$ and the decrease of average coordination number in these proto-Si:H films. Nevertheless, we cannot rule out the existence of dangling bonds in proto-Si:H, but think that floating bonds appear more likely than dangling bonds in this kind of material produced at the border line between a-Si:H and microcrystalline Si:H (μc-Si:H) [14]. Notice that the existence of floating bonds in a-Si is a rather disputed problem [26] and powerful evidence for it is still lacking. Our above statements on the one hand favor the concept of floating bond, on the other hand suggest that floating bonds may be experimentally detectable in the transitional materials between a-Si:H and μc-Si:H, such as proto-Si:H.

Finally, analogous to the FB model which has been successfully extended to crystalline semiconductors and dielectrics [27], we can also predict that the (single or multiple) TL model may be applicable for optical characterization and microstructure investigation of many other covalent and ionic materials, e.g., more than 100 widely different solids and liquids presented in references [18] and [19], no matter fully or partially crystalline and amorphous, provided the refractive-index dispersion behavior of these materials falls into the pattern described by the WD model and their subgap optical absorption is adequately small.

In summary, inherent characteristics within the TL model have been explored based on the fact that the TL-yielded subgap refractive index is found to obey remarkably the WD model. Consequently, we can attach new physical significance to the transition energy parameter of the TL model and gain insights into more applications of the TL model. Another criterion is proposed for judging the degree of QSE in amorphous/crystalline mixed-phase materials. Specific bond density, mass density, and coordination number information can also be revealed by the TL fitting parameters in combination with the WD model. These perspectives are favorable for deeper and wider usage of the TL model in many other covalent and ionic materials.

This work was supported in part by the Natural Science Foundation of China under contract No. 10125416, and Shanghai municipal major project of 03DJ14003.

References

1. G.E. Jellison, Jr., F.A. Modine, Appl. Phys. Lett. **69**, 371 (1996); G.E. Jellison, Jr., F.A. Modine, Appl. Phys. Lett. **69**, 2137 (1996)
2. A.R. Forouhi, I. Bloomer, Phys. Rev. B **34**, 7018 (1986)
3. A. Canillas, M.C. Polo, J.L. Andújar, J. Sancho, S. Bosch, J. Robertson, W.I. Milne, Diamond Relat. Mater. **10**, 1132 (2001)
4. M. Kildemo, R. Ossikovski, M. Stchakovsky, Thin Solid Films **313-314**, 108 (1998)
5. Y. Hayashi, G. Yu, M.M. Rahman, K.M. Krishna, T. Soga, T. Jimbo, M. Umeno, Appl. Phys. Lett. **78**, 3962 (2001)
6. K. Postava, M. Aoyama, T. Yamaguchi, H. Oda, Appl. Surf. Sci. **175-176**, 276 (2001)
7. G.E. Jellison, Jr., V.I. Merkulov, A.A. Puretzky, D.B. Geohegan, G. Eres, D.H. Lowndes, J.B. Caughman, Thin Solid Films **377-378**, 68 (2000)
8. H.J. Kim, Y.J. Cho, H.M. Cho, S.Y. Kim, C. Moon, G. Cho, Y. Kwon, AIP Conf. Proc. **683**, 171 (2003)
9. S. Adachi, H. Mori, Phys. Rev. B **62**, 10158 (2000)
10. Y.J. Cho, N.V. Nguyen, C.A. Richter, J.R. Ehrstein, B.H. Lee, J.C. Lee, Appl. Phys. Lett. **80**, 1249 (2002)
11. Z.G. Hu, J.H. Ma, Z.M. Huang, Y.N. Wu, G.S. Wang, J.H. Chu, Appl. Phys. Lett. **83**, 3686 (2003)
12. D. Amans, S. Callard, A. Gagnaire, J. Joseph, G. Ledoux, F. Huisken, J. Appl. Phys. **93**, 4173 (2003)
13. H. Chen, W.Z. Shen, Surf. Coat. Technol. (has been accepted, in press)

14. A. Fontcuberta i Morral, P. Roca i Cabarrocas, C. Clerc, Phys. Rev. B **69**, 125307 (2004)
15. N.V. Nguyen, J.P. Han, J.Y. Kim, E. Wilcox, Y.J. Cho, W. Zhu, Z. Luo, T.P. Ma, AIP Conf. Proc. **683**, 181 (2003)
16. A.S. Ferlauto, G.M. Ferreira, J.M. Pearce, C.R. Wronski, R.W. Collins, X. Deng, G. Ganguly, J. Appl. Phys. **92**, 2424 (2002)
17. M. Foldyna, K. Postava, J. Bouchala, J. Pištora, T. Yamaguchi, Proc. SPIE Int. Soc. Opt. Eng. **5445**, 301 (2004)
18. S.H. Wemple, M. DiDomenico, Jr., Phys. Rev. B **3**, 1338 (1971)
19. S.H. Wemple, Phys. Rev. B **7**, 3767 (1973)
20. I. Solomon, M.P. Schmidt, C. Sénémaud, M.D. Khodja, Phys. Rev. B **38**, 13263 (1988)
21. H.C. Lee, S.I. Lee, H. Lee, S.H. Choi, J.I. Ryu, J. Jang, J. Korean Phys. Soc. **39**, S30 (2001)
22. T.P. Chen, Y. Liu, M.S. Tse, O.K. Tan, P.F. Ho, K.Y. Liu, D. Gui, A.L.K. Tan, Phys. Rev. B **68**, 153301 (2003)
23. S. Nomura, T. Iitaka, X. Zhao, T. Sugano, Y. Aoyagi, Phys. Rev. B **59**, 10309 (1999)
24. K. Laaziri, S. Kycia, S. Roorda, M. Chicoine, J.L. Robertson, J. Wang, S.C. Moss, Phys. Rev. B **60**, 13520 (1999)
25. S.T. Pantelides, Phys. Rev. Lett. **57**, 2979 (1986)
26. M. Stutzmann, D.K. Biegelsen, Phys. Rev. Lett. **60**, 1682 (1988)
27. A.R. Forouhi, I. Bloomer, Phys. Rev. B **38**, 1865 (1988)